Heliyon 9 (2023) e18013

Contents lists available at ScienceDirect

Heliyon

journal homepage: www.cell.com/heliyon

Enhanced apoptosis of HCT116 colon cancer cells treated with extracts from *Calotropis gigantea* stem bark by starvation

Orakot Simanurak [a,1], Dumrongsak Pekthong [b,c,d,1], Julintorn Somran [e], Apirath Wangteeraprasert [f], Metawee Srikummool [g], Naphat Kaewpaeng [c,h], Supawadee Parhira [c,d,i,**], Piyarat Srisawang [a,c,j,*]

[a] *Department of Physiology, Faculty of Medical Science, Naresuan University, Phitsanulok 65000, Thailand*
[b] *Department of Pharmacy Practice, Faculty of Pharmaceutical Sciences, Naresuan University, Phitsanulok 65000, Thailand*
[c] *Center of Excellence for Innovation in Chemistry, Naresuan University, Phitsanulok 65000, Thailand*
[d] *Center of Excellence for Environmental Health and Toxicology, Faculty of Pharmaceutical Sciences, Naresuan University, Phitsanulok, 65000, Thailand*
[e] *Department of Pathology, Faculty of Medicine, Naresuan University, Phitsanulok, 65000, Thailand*
[f] *Department of Medicine, Faculty of Medicine, Naresuan University, Phitsanulok 65000, Thailand*
[g] *Department of Biochemistry, Faculty of Medical Science, Naresuan University, Phitsanulok 65000, Thailand*
[h] *Department of Pharmaceutical Chemistry and Pharmacognosy, Faculty of Pharmaceutical Sciences, Naresuan University, Phitsanulok 65000, Thailand*
[i] *Department of Pharmaceutical Technology, Faculty of Pharmaceutical Sciences, Naresuan University, Phitsanulok 65000, Thailand*
[j] *Center of Excellence in Medical Biotechnology, Faculty of Medical Science, Naresuan University, Phitsanulok 65000, Thailand*

ARTICLE INFO

Keywords:
Nutritional starvation
Colon cancer cells
Calotropis gigantea stem bark extract
Apoptosis
Reactive oxygen species

ABSTRACT

Calotropis gigantea stem bark extract, particularly the dichloromethane fraction (CGDCM), demonstrated the most potent antiproliferative effects on hepatocellular carcinoma HepG2 and colorectal HCT116 cells. The current study focused on enhancing the effectiveness of cancer treatment with CGDCM at concentrations close to the IC50 in HCT116 cells by reducing their nutrient supply. CGDCM (2, 4, and 8 μg/mL) treatment for 24 h under glucose conditions of 4.5 g/L without fetal bovine serum (FBS) supplementation or serum starvation (G+/F−), glucose 0 g/L with 10% FBS or glucose starvation (G−/F+), and glucose 0 g/L with 0% FBS or complete starvation (G−/F−) induced a greater antiproliferative effect in HCT116 cells than therapy in complete medium with glucose 4.5 g/L and 10% FBS (G+/F+). Nonetheless, the anticancer effect of CGDCM at 4 μg/mL under (G−/F−) showed the highest activity compared to other starvation conditions. The three starvation conditions showed a significant reduction in cell viability compared to the control (G+/F+) medium group, while the inhibitory effect on cell viability did not differ significantly among the three starvation conditions. CGDCM at 4 μg/mL in (G−/F−) medium triggered apoptosis by dissipating the mitochondrial membrane potential and arresting cells in the G2/M phase. This investigation demonstrated that a decrease in intracellular ATP and fatty acid levels was associated with enhanced apoptosis by treatment with CGDCM at 4 μg/mL under (G−/F−) conditions. In addition, under (G−/F−), CGDCM at 4 μg/mL increased levels of

* Corresponding author. Department of Physiology, Faculty of Medical science, Naresuan University, Phitsanulok 65000, Thailand.
** Corresponding author. Department of Pharmaceutical Technology, Faculty of Pharmaceutical Sciences, Naresuan University, Phitsanulok 65000, Thailand.
E-mail addresses: supawadeep@nu.ac.th (S. Parhira), piyarats@nu.ac.th (P. Srisawang).
[1] These authors contributed equally to this work.

https://doi.org/10.1016/j.heliyon.2023.e18013
Received 14 February 2023; Received in revised form 26 June 2023; Accepted 5 July 2023
Available online 7 July 2023

reactive oxygen species (ROS) and was suggested to primarily trigger apoptosis in HCT116 cells. Thus, *C. gigantea* extracts may be useful for the future development of alternative, effective cancer treatment regimens.

1. Introduction

Despite being recognized as one of the most prevalent malignancies, the mortality rate of colon cancer is also one of the highest in the world [1,2]. The colorectal cancer (CRC) incidence is reported to be among the top three cancer rates in both men and women and the second highest when men and women are combined [3]. Chemotherapeutic medicines, such as 5-fluorouracil (5-FU), provide a higher risk of severe adverse effects on normal tissues, hence limiting their therapeutic efficacy [4]. Consequently, significant progress in the discovery of potential cancer therapies has been focused on the development of plant extracts as alternative therapeutic regimens to improve their effectiveness and counteract cytotoxicity in normal cells.

Normal cells rely on nutrition as the primary substrate for energy metabolism via the mitochondrial citric acid cycle, which converts glucose into adenosine triphosphate (ATP). Additionally, glucose is required for the biosynthesis of several macromolecules that are essential for cell growth [5]. In addition, fatty acids (FAs) function as energy substrates for cell development signaling molecules [6–8]. In contrast to normal cells, cancer cells have a modified metabolism, including increased glucose absorption, glutaminolysis, and fatty acid production, as an adaptation for tumor cell growth and survival [9]. The metabolic shift of cancer cells, or the "Warburg effect," demonstrates enhanced anaerobic metabolism of ATP synthesis under conditions without dependence on the supply of oxygen that leads to increased lactate production. Overexpression of transient receptor potential channel 5 (TRPC5) in breast cancer cells enhances glucose absorption via glucose transporter protein (GLUT) upregulation, which is correlated with the PI3K/Akt pathway and leads to enhanced breast carcinogenesis [10]. The overexpression of GLUT1 in gastric cancer cells improves glucose uptake and consumption, elevates lactate and ATP production, and ultimately stimulates cell proliferation [11]. In addition, the overexpression of sodium-glucose transporter 2 (SGLT2) in breast cancer [12] and human liver cancer cells [13] contributes significantly to cancer proliferation and progression.

Nutrient deprivation has a cytotoxic effect on cancer cells [14–17]. Decreasing glucose absorption by downregulating GLUT-1 inhibited the development of colon cancer cells [18]. In addition, glucose restriction promotes the anticancer efficacy of numerous anticancer therapy regimens. Secalonic acid D, a xanthone derivative derived from the culture medium of marine-derived *Penicillium oxalicum,* exhibits antiproliferative activity against human pancreatic cancer PANC-1 cells under glucose deficiency conditions by selectively suppressing the mitochondrial oxygen consumption rate of oxidative phosphorylation [19]. Low glucose medium improved the sensitivity of rat glioma, human glioma, and human neuroblastoma cells to chemotherapeutic agents [20]. Metformin induced apoptosis in hepatocellular carcinoma HepG2/C3A and HuH-7 cells under glucose-depleted conditions [21]. In addition to glucose, de novo fatty acid synthesis is a key source of energy for membrane formation and the reducing equivalent nicotinamide adenine dinucleotide phosphate (NADPH) for the antioxidant system, hence promoting cell viability [22,23]. Fatty acid synthesis inhibition occurs by inhibiting fatty acid β-oxidation (FAO) and fatty acid synthase (FASN) activities, resulting in apoptotic cell death [24–27]. Therefore, nutrient restriction is strongly suggestive of an antiproliferative treatment for cancers and may have prospectively enhanced anticancer efficacy in future cancer therapeutic research.

Fetal bovine serum (FBS) is recognized as a nutrient-rich supplement to culture media that is essential for promoting cell metabolism, growth, and proliferation [28]. Following serum deprivation, head and neck squamous cell carcinoma proliferation and migration were significantly reduced as a result of abnormal cell growth, proliferation, and progression gene expression [29]. Short-term starvation increased the toxicity of the chemotherapeutic agent oxaliplatin in mice bearing CT26 colon carcinoma cells and exhibited additive cytotoxic effects in colon cancer cell lines [30]. As a result, therapeutic development focused on the nutritional supply of cancer cells has been highlighted as a prospective anticancer strategy.

Numerous studies have demonstrated that natural extracts are effective anticancer treatments due to their safety and practicability in preclinical cancer therapy investigations [31]. *Calotropis gigantea* (*C. gigantea*) is a member of the Apocynaceae family and the Asclepiadaceae subfamily. It is a native plant of various Eastern and Southeast Asian nations, including China, Thailand, Malaysia, the Philippines, Cambodia, Indonesia, Laos, India, and Sri Lanka [32]. In Thailand, it is commonly known as "*Rak*". Several parts of *C. gigantea*, including the leaves, flowers, stem bark, root bark, and latex, are extensively used in folk medicine to treat illnesses, and it has preventive properties against the proliferation of numerous types of cancer cells [33–37]. Currently, the effectiveness of monotherapy against cancer cells remains severely limited. Combinations of *C. gigantea* CGDCM extract and 5-FU at doses below their respective IC50 were discovered to have significant therapeutic potential [37]. Therefore, it seems reasonable to hypothesize that combining CGDCM extract from *C. gigantea* stem bark with nutritional disruption will enhance anticancer therapeutic results.

According to current knowledge, *C. gigantea* CGDCM stem bark extract has the potential to be one of the most promising cancer therapy regimens for future cancer treatment research. The objective of our study focused on enhancing the anticancer activity of nutrient starvation on the stem bark CGDCM extract fraction of *C. gigantea* at low concentrations. Our results will provide the basis for the application of alternative anticancer therapeutic regimens comprising plant extracts and nutritional deprivation approaches against cancer cells.

2. Materials and methods

2.1. Plant material and sample preparation

The collection and identification of the stem bark of *C. gigantea*, concomitantly with procedures including the extraction, fractionation, and quantitative analysis of total contents of several phytochemicals in CGDCM, which was the sample used in this research, were performed in our previous report elsewhere [37]. Briefly, the powdered, shade-dried stem bark of *C. gigantea* was extracted with ethanol at 95% using ultrasonic assistance to obtain the crude extract and subsequently exposed to liquid−liquid partition between water and dichloromethane to obtain the CGDCM fraction. The CGDCM sample was kept in a refrigerator (4 ± 3 °C) until use. Plant collection and use of the collected plants for research purposes was approved to comply with the Plant Varieties Protection Act B.E. 2542 (1999) Section 53 (permission number 0278) from the Department of Agriculture, Ministry of Agricultural and Cooperatives, Thailand.

2.2. Quality control of CGDCM and characterization of calactin

Quality control of the tested sample, the CGDCM fraction, was performed in our previous report [37] by characterizing and measuring the content of calotropin in the sample by high-performance liquid chromatography (HPLC).

In this study, one more cardenolide possessing anticancer activities, calactin, was characterized through high-resolution mass spectrometry (HRMS) by using an Agilent 6540 UHD LCMS instrument. CGDCM was dissolved in methanol (MS grade, 1 mg/mL) and then injected (10 μL) into a Phenomenex Luna® 3 μm C18 column (batch 5292-0075, dimensions 150 mm × 4.6 mm i.d., part number 00F−4251-E0, serial number H5-150810) maintained the temperature of autosampler and column at 4 and then 25 °C, respectively. A gradient system that included 0.1% formic acid-water solution and 0.1% formic acid-acetonitrile solution (0–95% acetonitrile, 30 min) was used as the mobile phase. Throughout the analysis time, a constant flow rate of 0.8 mL/min was used. The detector used in this procedure was the negative mode (m/z range 200–800) of the dual electrospray ionization setup with a 30 psi nebulizer pressure (N2), a 10 L/min drying gas flow rate, and a 350 °C temperature. The retention time in the base peak chromatogram (BPC) and mass spectra of CGDCM were used to characterize the existence of calactin in CGDCM compared to those of the blank (methanol) and calactin standard.

2.3. Culture of HCT116 cells

HCT116 colon cancer cells were purchased from the RIKEN BRC CELL BANK (RCB2979, Japan) and cultured in McCoy's 5A (Corning, USA) supplemented with 10% FBS (Gibco, USA) and 1% Antibiotic-Antimycotic (Gibco, USA) as complete growth medium. Normal human fibroblast IMR-90 cells (JCRB9054) (JCRB Cell Bank, Japan) were cultured in complete growth media of 10% FBS and 1% Antibiotic-Antimycotic supplement in DMEM (Corning, USA). A CO_2 incubator set at a temperature of 37 °C and 5% CO_2 was used for cultured cells.

Cells were divided into 4 groups for the treatments: Group 1) vehicle complete medium with 4.5 g/L glucose and 10% FBS: (G+/F+), Group 2) serum starvation with 4.5 g/L glucose and 0% FBS: (G+/F−), Group 3) glucose starvation with 0 g/L glucose and 10% FBS: (G−/F+) and Group 4) complete starvation with 0 g/L glucose and 0% FBS: (G−/F−).

2.4. Cell proliferation assay

Cell proliferation was determined by the cell viability assay dye 3-(4,5-dimethylthiazol-2-yl)-2,5-diphenyltetrazolium bromide (MTT) (Merck, Germany). Briefly, after 24 h of treatment with various concentrations of CGDCM in complete (G+/F+) medium and under starvation conditions, harvested cells were incubated for 4 h with MTT solution at 2 mg/mL at 37 °C. The yellow color of MTT is converted into the violet color of formazan crystals from the activity of the mitochondrial reductase enzyme. The crystal was then dissolved in dimethyl sulfoxide (DMSO) (Sigma, USA), and the cell viability levels were determined using a 595 nm OD microplate reader (Synergy, BioTek, USA). GraphPad Prism 9 software was used to calculate cell viability percentages in comparison to (G+/F+) medium.

2.5. Detection of cell proliferation by crystal violet assay

Cell proliferation was examined using crystal violet (SIGMA, USA). Briefly, after treatment, crystal violet in 70% ethanol was applied to the cells for 30 min of incubation. Stained cells were measured with an inverted optical microscope (IX71, Olympus, Japan).

2.6. Wound healing assay

After reaching a cell monolayer density of 80% in a 12-well plate (Corning, USA), the gap between cells was created by scraping, and then the gap distance was measured using an inverted optical microscope (IX71, Olympus, Japan) with CellSens standard (Ver.2.3) software. The images were captured at 4× magnification.

2.7. Flow cytometric determination of apoptosis

After 24 h of treatment, apoptosis was evaluated by double labeling cells with Annexin V/Alexa Fluor 488 conjugate (A13201, Invitrogen, USA) and propidium iodide (PI) (P3566, Invitrogen, USA). During early apoptosis, Annexin V stains phosphatidylserine (PS) in the outer membrane. PI can enter the cell and attach to double-stranded DNA when the cell membrane becomes permeable. Cells in the late apoptosis stage were stained with both Annexin V and PI. The apoptotic cells were quantified with CytoFLEX flow cytometry and CytExpert software (Version 2.4.0.28) (Beckman Coulter, USA) and calculated as percentages using GraphPad Prism9 software.

2.8. Measurement of the cell cycle by flow cytometry

After cells were treated for 24 h, harvested cells were fixed with cold 70% ethanol for 4 h at 4 °C. RNase A (AMRESCO, OH, USA) and PI were applied to cells before the cell cycle of stained cells was detected by CytoFLEX flow cytometry and analyzed using CytExpert software.

2.9. Reduction in mitochondrial membrane potential detected by flow cytometry and fluorescence microscopy

Mitochondrial membrane potential (MMP) is a key apoptosis regulator [38,39]. To measure MMP in the apoptosis pathway, after cells were treated for 24 h, 10 μg/mL 5,5′,6,6′-tetrachloro-1,1′,3,3′-tetraethylbenzimidazolylcarbocyanine iodide (JC-1; CBIC2(3)) (Invitrogen, USA) was applied to harvested cells. MMP levels were detected by CytoFLEX flow cytometry and analyzed using CytExpert software.

For visualization of MMP by fluorescence microscopy, after treating cells, 4% formaldehyde was applied and incubated for 15 min at room temperature to fix cells, followed by staining cells with 4′,6-diamidino-2-phenylindole, dihydrochloride (DAPI) (Invitrogen, USA) and JC-1 dye. Finally, visualization of the fluorescence of stained cells was performed with fluorescence microscopy (BX53F2, Olympus Corporation, Japan).

2.10. Intracellular ATP level determination

A Luminescent ATP detection assay kit (ab113849: Abcam, USA) was used to measure the level of intracellular ATP. After treating

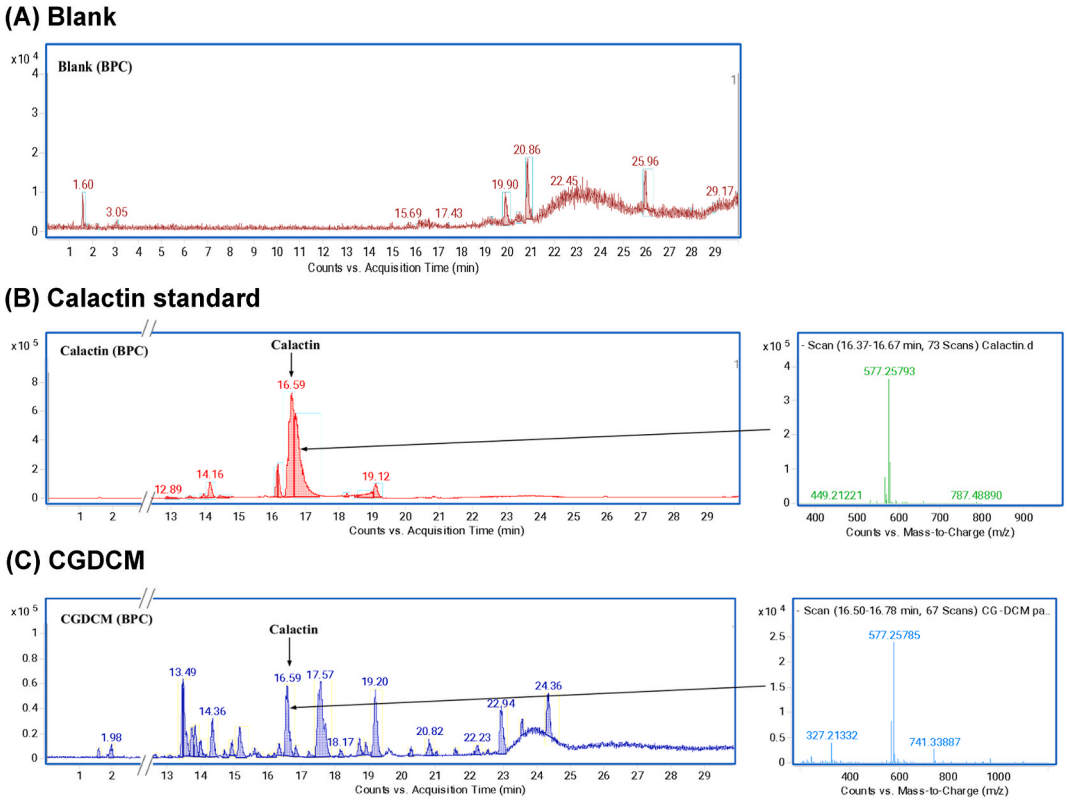

Fig. 1. Base peak chromatograms and mass spectra of (A) Blank, (B) calactin standard and (C) CGDCM.

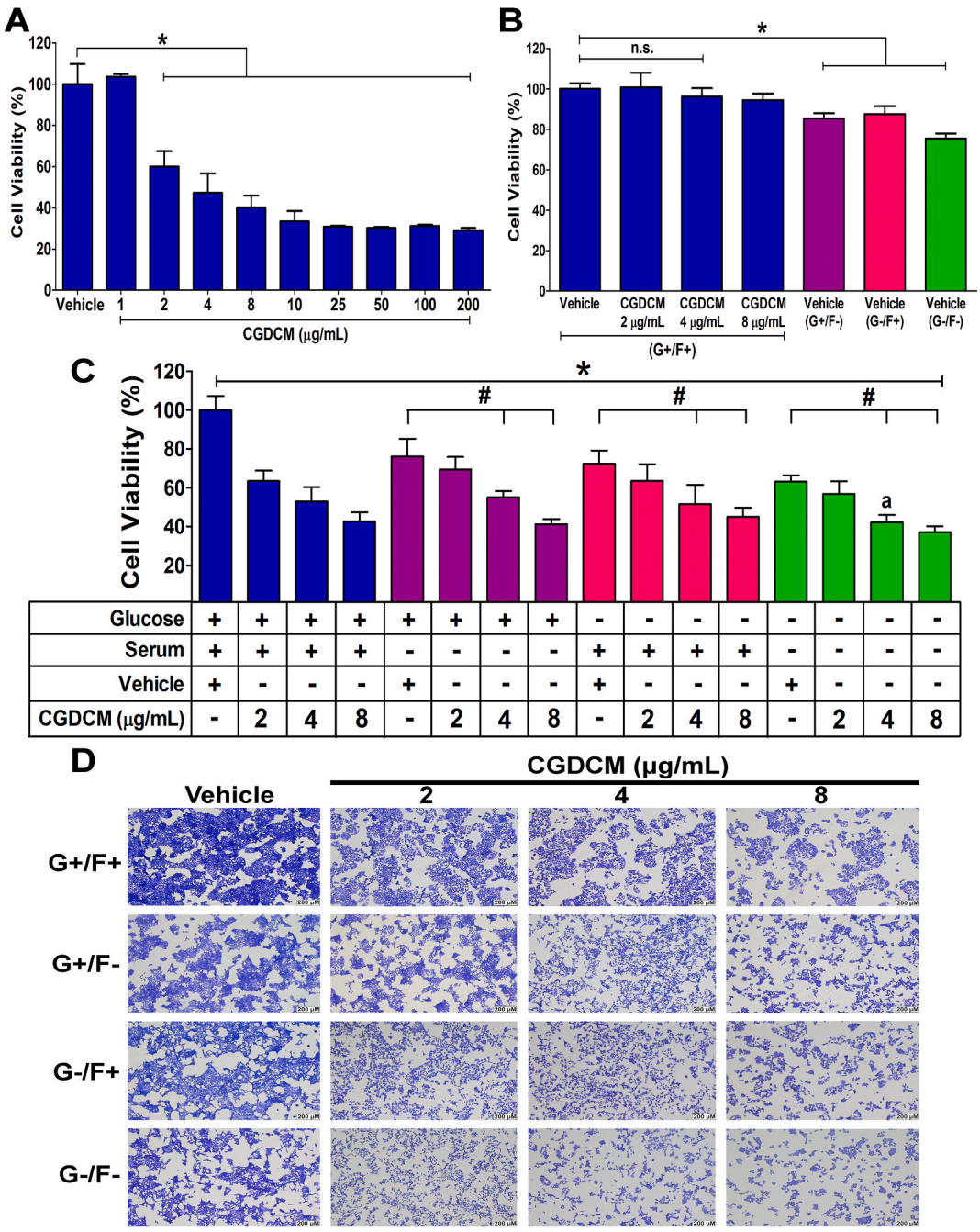

Fig. 2. The effects of the CGDCM extract fraction from the stem bark of *C. gigantea* against the HCT116 cytotoxic effect after 24 h of incubation. (A) The MTT assay was used to measure the inhibitory effect of CGDCM in complete medium (G+/F+) on HCT116 cells, and (B) IMR-90 fibroblasts were treated with CGDCM at 2, 4, and 8 μg/mL in complete medium (G+/F+) and vehicle starvation conditions: serum starvation (G+/F−), glucose starvation (G−/F+), and complete starvation (G−/F−). (C) Cell viability of HCT116 cells treated with CGDCM at 2, 4, and 8 μg/mL under (G+/F+), (G+/F−), (G−/F+), and (G−/F−) conditions. (D) Representative cell viability images were obtained using the crystal violet assay to determine HCT116 cell viability after treatment with CGDCM under (G+/F+) and starvation conditions. 0.8% DMSO in (G+/F+) and three distinct starvation media represent the vehicle control. The data are presented as the mean ± SD, and the significant differences were analyzed with one-way ANOVA using Tukey's HSD test at *; $p < 0.05$ versus the vehicle group in (G+/F+) medium. n = 3. (For interpretation of the references to color in this figure legend, the reader is referred to the Web version of this article.)

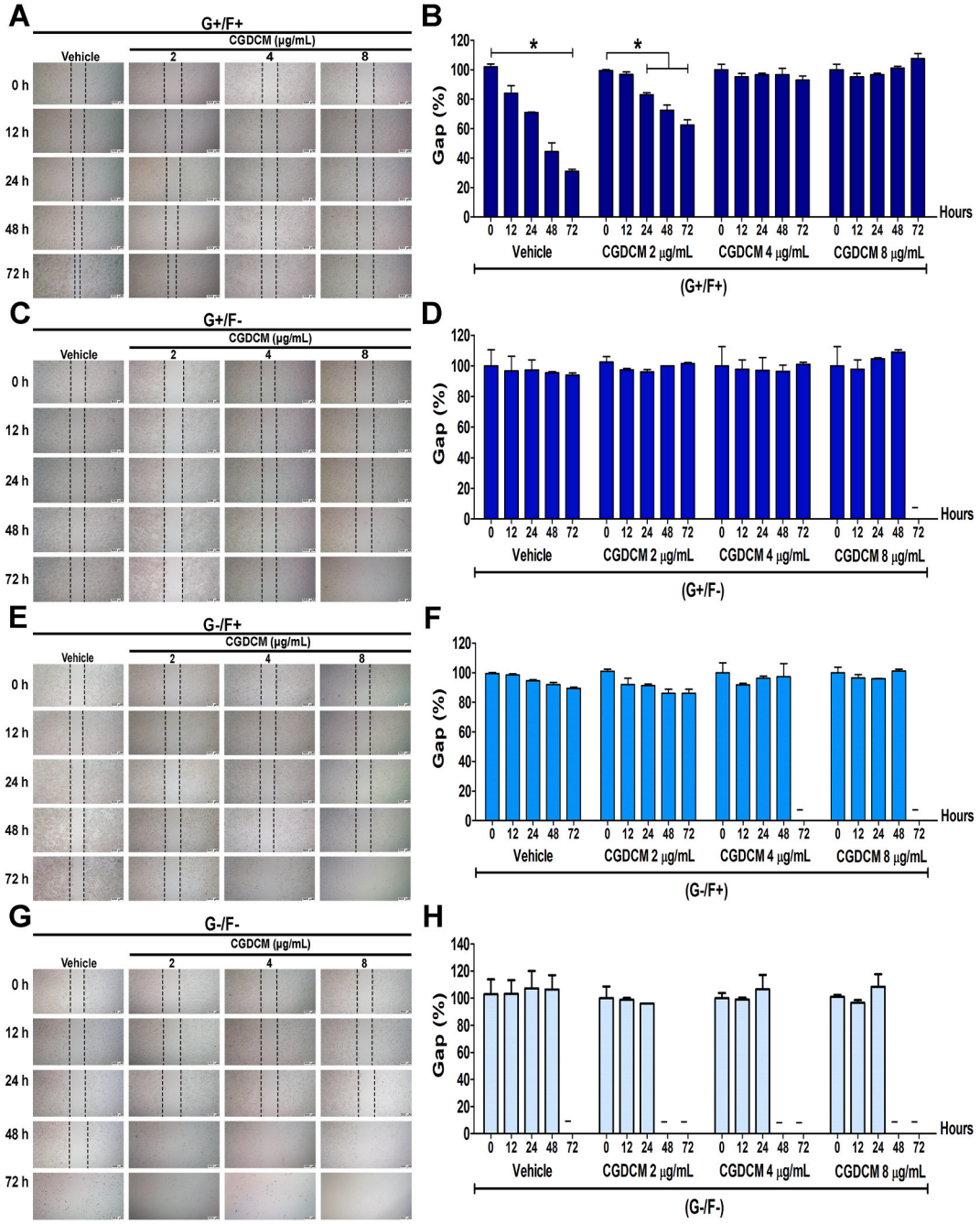

Fig. 3. The suppression effects on the migration ability of the CGDCM extract fraction from the stem bark of *C. gigantea* in HCT116 cells under starvation conditions. Representative morphologies of the wound-healing determination of migration and a percentage of the migration gap were obtained at 0, 12, 24, 48, and 72 h of CGDCM under (A, B) (G+/F+) medium and three distinct starvation media, (C, D) (G+/F−), (E, F) (G−/F+), and (G, H) (G−/F−). Scale bar = 500 μm. 0.8% DMSO in (G+/F+) and three distinct starvation media represent the vehicle control. The data are presented as the mean ± SD, and the significant differences were analyzed with one-way ANOVA using Tukey's HSD test at *; $p < 0.05$ versus the 0-h vehicle media group. n = 3.

and harvesting cells, the luciferase enzyme and luciferin were added to cells and incubated for 10 min at room temperature under light protection. The luminescence signal was detected using a microplate reader (SpectraMax iD3, Molecular Devices, USA).

2.11. Fatty acid level determination

A nonesterified free fatty acid (NEFA) colorimetric assay kit (E-BC-K013-M: Elabscience, USA) was applied to measure intracellular fatty acid concentrations after treating and harvesting cells, following the manufacturer's instructions. A microplate reader at 715 nm optical density (OD) was used for this procedure.

2.12. Measurement of reactive oxygen species (ROS) production by flow cytometry and fluorescence microscopy

2′,7′-Dichlorodihydrofluorescein diacetate (H_2DCFDA) (Invitrogen, USA) was applied to stain cells to measure the formation of ROS according to the principle of the conversion of nonfluorescent H_2DCFDA into highly fluorescent 2′,7′-dichlorofluorescein (DCF). Following 24 h of treatment, cells were harvested and incubated in a CO_2 incubator with H_2DCFDA for 45 min under light protection. CytoFLEX flow cytometry was used to measure the DCF fluorescence signals, and CytExpert software was used for data analysis.

For fluorescence microscopy detection of ROS production, 4% formaldehyde was applied and incubated for 15 min at room temperature to fix cells, followed by the addition of H_2DCFDA and counterstaining with DAPI. Finally, the fluorescence of stained cells was visualized by fluorescence microscopy.

2.13. Statistical analysis

Data are presented as the mean ± SD, and the statistical significance of differences between the experimental and control groups at $p < 0.05$ was analyzed with one-way analysis of variance (ANOVA) or Student's *t*-test with Tukey's post hoc test. Graph Prism Software version 9 was used to analyze all data.

3. Results

3.1. Characterization of calactin in CGDCM

The quality control of CGDCM was previously performed and reported by using HPLC to measure the content of calotropin (6.2 ± 0.32 mg calotropin/10 g CGDCM) [37,40]. Calactin, a cardenolide possessing anticancer activities, was identified in CGDCM and characterized by using HRMS by comparing BPC and MS spectra to those of the blank and calactin standard, as shown in Fig. 1A–C. It was found that the observed $[M + HCOO]^-$ with *m/z* 577.25785 (the differences from calculated mass and standard calactin were 19.83 and 0.14 ppm, respectively) in the CGDCM sample at the retention time 16.37–16.67 min were similar to those of the calactin standard ($C_{29}H_{40}O_9$, calculated mass 577.2693, observed $[M + HCOO]^-$, *m/z* 577.25793; the difference from calculated mass was 19.69 ppm) with the same retention time of approximately 16.50–16.78 min. The results supported the existence of calactin in CGDCM.

3.2. The antiproliferative effects on HCT116 cells treated with the extract fractions from the stem bark of C. gigantea

We previously reported the cytotoxic effects of four extract fractions, the crude ethanolic extract (CGEtOH), dichloromethane (CGDCM), ethyl acetate (CGEtOAc), and water (CGW), from the stem bark of *C. gigantea*. When HCT116, HT-29, and HepG2 cells were treated with CGDCM for 24 h, it demonstrated the highest anticancer activity compared to other fractions [37,40]. Consistent with the previous study, the current examination indicated that CGDCM had an anticancer effect with an IC50 of 4.75 ± 1.70 μg/mL after 24 h on HCT116 cells (Fig. 2A). In consideration of this, we included CGDCM in the current study to investigate the improved anticancer efficacy against HCT116 cells under starvation conditions.

The normal fibroblast IMR-90 cells treated with CGDCM at doses of 2, 4, and 8 μg/mL, which were below and above the IC50 in complete medium (G+/F+) (Fig. 2B), demonstrated that after 24 h of incubation, CGDCM had no cytotoxic effect on normal fibroblast cells, whereas vehicle starvation medium treatment, (G+/F−), (G−/F+), and (G−/F−), induced significant cytotoxicity compared to the vehicle (G+/F+) group.

Compared to the vehicle (G+/F+), vehicle (G−/F−), and CGDCM at 4 μg/mL in (G+/F+), the inhibitory effect on cell viability of CGDCM at 4 μg/mL in (G−/F−) starvation was significantly more effective on HCT116 cells (Fig. 2C). As shown in Fig. 2D, crystal violet staining indicated the antiproliferative activity of CGDCM under conditions of nutrient deprivation. Consequently, this finding suggests that complete starvation (G−/F−) enhances the antiproliferative activity of CGDCM on HCT116 cells, although it has a lesser effect on normal cells.

3.3. The inhibitory effect on the cell migration ability of HCT116 cells after treatment with the CGDCM extract fraction from the stem bark of C. gigantea

A wound healing assay was used to investigate the inhibitory effect on HCT116 cell migration under starvation conditions at 0, 12, 24, 48, and 72 h. As shown in Fig. 3A and B, CGDCM at 2, 4, and 8 μg/mL in complete medium (G+/F+) inhibited the migration of

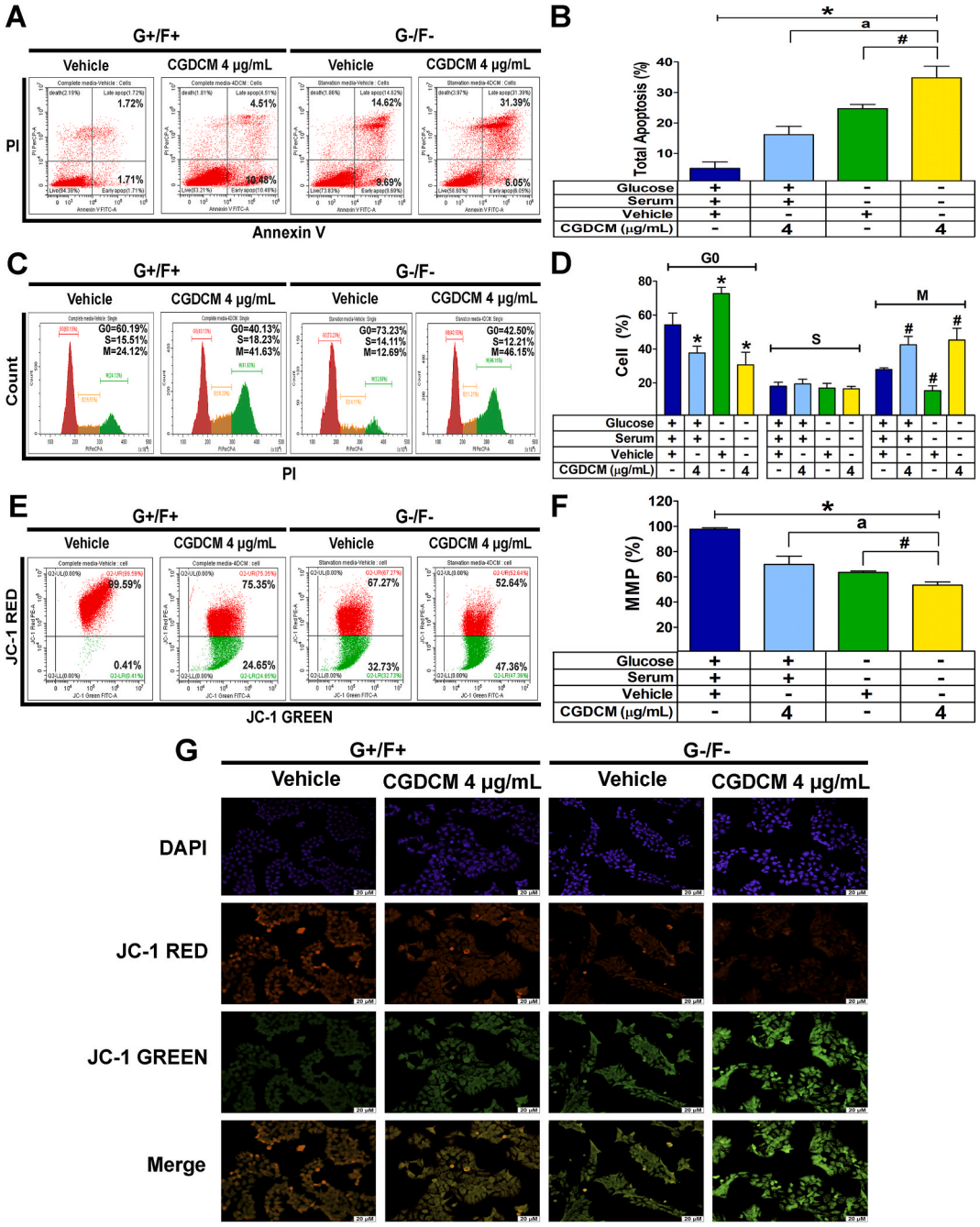

Fig. 4. Apoptotic induction, cell cycle arrest, and MMP dissipation activities followed treatment of HCT116 cells with the CGDCM extract fraction from the stem bark of *C. gigantea* under starvation conditions after 24 h of incubation. Cells were treated with 4 μg/mL CGDCM under (G−/F−) starvation compared to vehicle (G+/F+) medium. (A) Representative apoptosis of flow cytometry examination staining with annexin-V and PI. (B) The histogram displays the percentage of total apoptotic cells. (C) Representative flow cytometry analysis of phases of the cell cycle. (D) The histogram displays the percentage of cell cycle phases. *; $p < 0.05$ versus the vehicle (G+/F+) medium in G0/G1 phase and #; $p < 0.05$ versus the vehicle (G+/F+) medium in G2/M phase. (E) Representative flow cytometry analysis of MMP. (F) The histogram displays the percentage of MMP. (G) Representative fluorescent images of MMP stained by JC-1 and apoptotic cell nuclei stained by DAPI. Scale bar = 20 μm. DMSO (0.8%) in (G+/F+) and (G−/F−) medium represents the vehicle control. The data are presented as the mean ± SD, and the significant differences were analyzed with one-way ANOVA using Tukey's HSD test at *; $p < 0.05$ versus the vehicle (G+/F+) medium. n = 3.

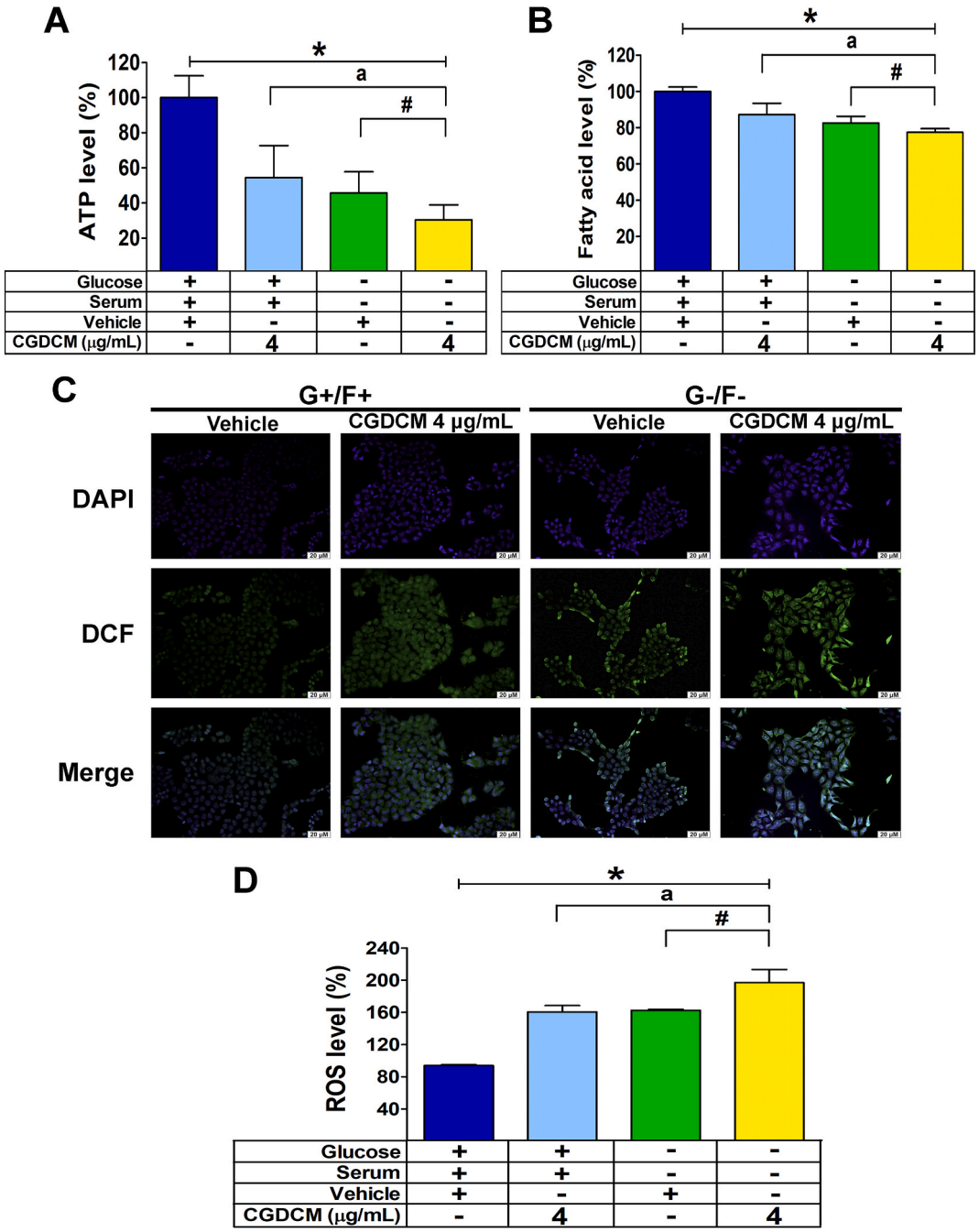

Fig. 5. CGDCM extract fraction of *C. gigantea* stem bark on intracellular ATP, fatty acid, and ROS levels under starvation conditions incubated for 24 h in HCT116 cells. The histogram depicts the percentage of (A) ATP and (B) fatty acid levels. (C) Representative image of ROS generation detected by staining with DCF and detected by fluorescence microscopy, scale bar = 20 μm. (D) The histogram demonstrates the percentage of ROS production. 0.8% DMSO in (G+/F+) and (G−/F−) medium represents the vehicle control. The data are presented as the mean ± SD, and the significant differences were analyzed with one-way ANOVA using Tukey's HSD test at *; $p < 0.05$ versus the vehicle group in (G+/F+) medium. n = 3.

HCT116 cells in comparison to vehicle (G+/F+). CGDCM at 2, 4, and 8 μg/mL under all starvation conditions, (G+/F−), (G−/F+), and (G−/F−), inhibited the migration of HCT116 cells relative to their own vehicle medium (Fig. 3C-H). Thus, the suppressive effect on cell migration verified the increased antiproliferative action of CGDCM during nutrient deprivation. In subsequent experiments, CGDCM at 4 μg/mL in the (G−/F−) condition was applied to determine its anticancer activity.

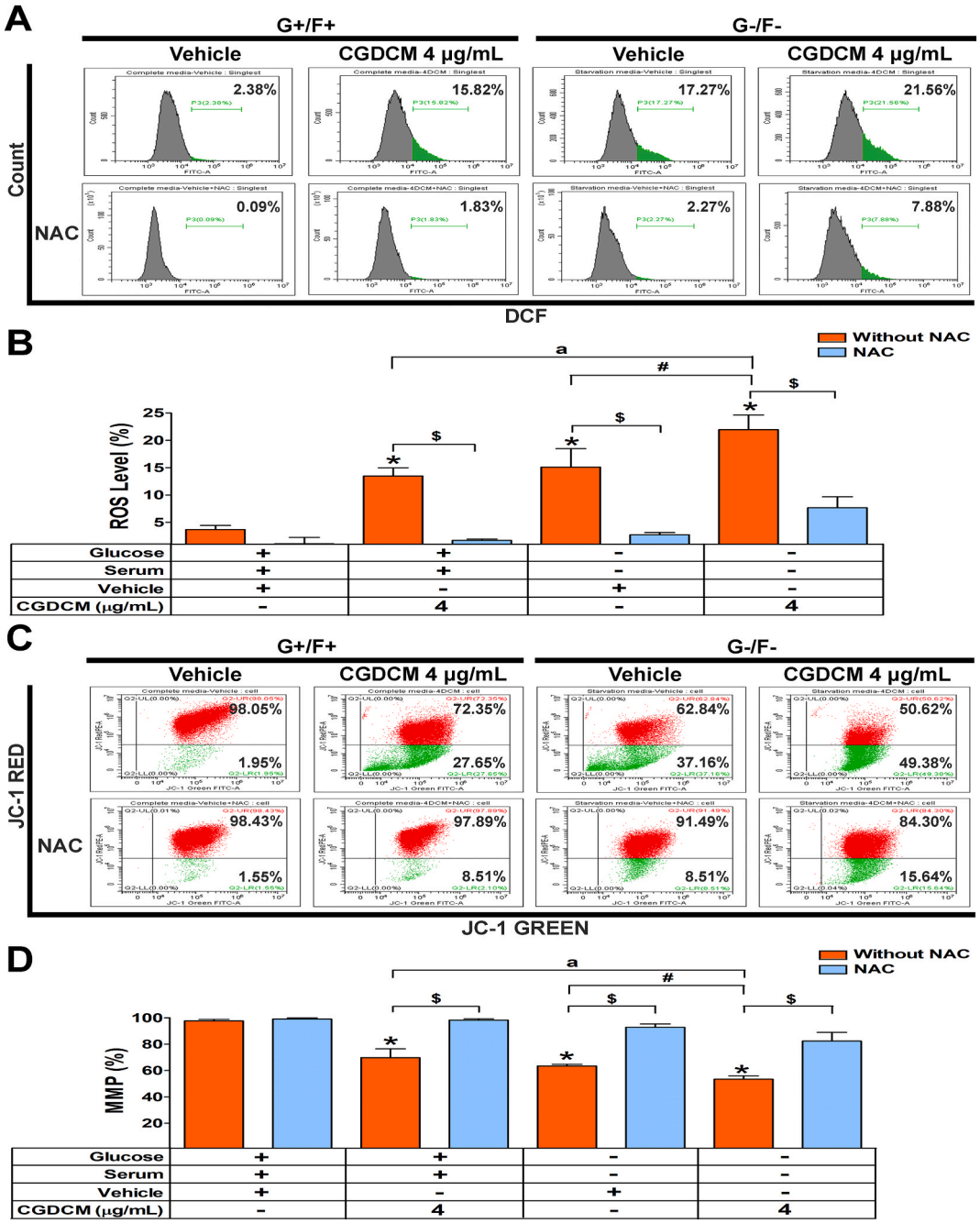

Fig. 6. The effects of the CGDCM extract fraction of the stem bark of *C. gigantea* under starvation conditions for 24 h on ROS generation and dissipation of MMP using N-acetylcysteine (NAC) preincubation for 2 h in HCT116 cells. Cells were treated with 4 μg/mL CGDCM under (G−/F−) starvation compared to vehicle (G+/F+) medium. (A) Representative flow cytometry analysis of ROS generation. (B) The histogram demonstrates the percentage of ROS production. (C) Representative flow cytometry determination of MMP by JC-1 staining. (D) The histogram demonstrates the percentage of MMP. DMSO (0.8%) in (G+/F+) and (G−/F−) medium represents the vehicle control. The data are presented as the mean ± SD, and the significant differences were analyzed with one-way ANOVA using Tukey's HSD test at *; $p < 0.05$ versus the vehicle (G+/F+) group. $n = 3$.

3.4. Apoptosis and cell cycle arrest in HCT116 cells after treatment with the CGDCM extract fraction from the stem bark of C. gigantea under complete starvation

Flow cytometry analysis was used to analyze the induction of apoptosis following treatment with CGDCM under starvation conditions and is shown in Fig. 4A and B. Treatment of HCT116 cells with CGDCM at 4 μg/mL under (G−/F−) starvation significantly increased the percentage of total apoptosis compared to vehicle (G+/F+) and CGDCM in (G+/F+), and vehicle (G−/F−) conditions. In addition, cell cycle analysis showed that 4 μg/mL CGDCM in both (G+/F+) and (G−/F−) medium arrested cells in the G2/M phase, but (G−/F−) starvation arrested cancer cells in the G0/G1 phase (Fig. 4C and D). In addition, CGDCM at 4 μg/mL in (G−/F−) starvation significantly enhanced the loss of mitochondrial membrane potential (MMP) compared to vehicle (G+/F+), CGDCM in (G+/F+), and vehicle (G−/F−) conditions, as shown in Fig. 4E–G. These findings suggest that complete starvation appears to enhance the effect of CGDCM on mitochondrial membrane potential loss-mediated apoptosis and cell cycle arrest in HCT116 cells.

3.5. Under complete starvation, CGDCM induced apoptosis in HCT116 cells by modulating ATP, fatty acid, and ROS production

Fig. 5A demonstrates that after 24 h of incubation, CGDCM treatment in HCT116 cells under (G−/F−) starvation significantly decreased ATP levels compared to vehicle (G+/F+), CGDCM in (G+/F+), and vehicle (G−/F−) conditions. As depicted in Fig. 5B, the decrease in fatty acid levels following CGDCM treatment in HCT116 cells under (G−/F−) deprivation displayed a suppression pattern similar to that of the ATP assay.

Fig. 5C and D demonstrate that significantly elevated ROS production was observed following treatment of HCT116 cells with 4 μg/mL CGDCM during (G−/F−) starvation compared to vehicle (G−/F−), CGDCM 4 μg/mL in (G+/F+), and vehicle (G−/F−) conditions. N-acetylcysteine (NAC) was applied to inhibit ROS production to demonstrate a relationship between ROS and apoptosis in cancer cells [41]. ROS generation recovered to control levels after HCT116 cells were pretreated with NAC followed by treatment with CGDCM under (G−/F−) deprivation for 24 h (Fig. 6A and B). Similarly, NAC significantly inhibited the dissipation of MMP produced by treatment with 4 μg/mL CGDCM in the (G−/F−) condition (Fig. 6C and D). The data indicate that ROS generation is important for the increased apoptotic effect of CGDCM on HCT116 cells during complete starvation (G−/F−).

4. Discussion

The extraction, fractionation, and quality control of CGDCM were performed as described in our previous report [37]. The content of calotropin was determined and used as a bioactive marker for the anticancer activity of CGDCM. In this study, calactin, an isomer of calotropin, which has been reported to possess stronger anticancer activity than calotropin, was also identified and characterized by using HRMS to confirm its existence in CGDCM. However, due to the limitation of the amount of calactin standard, the determination of calactin content in CGDCM could not be performed in this study.

Cancer cells have high glucose consumption, resulting in lower glucose levels in the tumor's surroundings than in normal tissues [42,43]. In addition, glucose deprivation in a tumor environment is caused by abnormal angiogenesis and over cell proliferation that exceeds the energy supply, resulting in hypoxia and starvation that consequently enhance glycolysis independent of the availability of oxygen supply, as recognized by the Warburg effect [43,44]. It has been suggested that a high blood glucose microenvironment upregulates the expression of sterol regulatory element-binding protein 1 (SREBP1), resulting in accelerated cell proliferation and cancer progression compared to normal blood glucose levels [45]. Increased glucose metabolism via glycolysis upregulates the expression of transient receptor potential channel 5 opposite strand (TRPC5OS) mRNA, leading to activated cancer cell proliferation and tumorigenesis in breast cancer cells [10]. Increased glucose uptake and glycolytic flux reported in prostate cancer cells have been suggested to be associated with an upregulation of glucose transporter protein-1 (GLUT1) expression [46]. In breast cancer cells, a high glucose condition increased the expression of the anti-apoptotic protein Bcl-2, which promoted angiogenesis and proliferation compared to a normal glucose condition [47].

In this regard, a number of studies have demonstrated that cancer cells exposed to conditions of low glucose availability or in the presence of free glucose are more susceptible to cell death than normal cells, suggesting that nutritional fasting inhibits cancer cell proliferation and promotes apoptosis [48,49]. In addition, inhibiting glucose uptake by sodium-glucose transporter 2 (SGLT2), whose expression level is upregulated in breast cancer tissue compared to normal breast tissue, suppressed cancer proliferation through the AMPK/mTOR pathway [12]. Nutrient deprivation (lack of glucose, glutamine, and calcium) inhibited C6 glioma stem-like cell development and increased apoptosis [48]. Glucose deprivation upregulates the expression of the proapoptotic proteins Bim, Bid, Bax, caspase-3, and ApaF−1 while downregulating the expression of the antiapoptotic protein Bcl-2, stimulating the apoptosis pathway in breast cancer cells [50]. Glucose deprivation in human malignant mesothelioma MS1 and H513 cells decreased total ATP levels, resulting in decreased cell growth and activation of apoptosis [51]. Hepatocellular carcinoma HepG2/C3A and HuH-7 cells exhibited apoptosis with G0/G1 cell cycle arrest when cultured in the absence of glucose [21]. In addition, in the absence of glucose, increased lactate production from glycolysis suppresses protease activity that decomposes the extracellular matrix for cancer cell proliferation, resulting in the inhibition of peptides and amino acid liberation necessary for cancer cell energy production [43]. Therefore, glucose deprivation may be a possible anticancer therapeutic strategy. Consistent with prior findings, our data demonstrate that glucose starvation inhibited the growth of HCT116 colorectal cancer cells.

Increased ROS production has been considered a mechanism for triggering apoptosis in response to glucose deprivation [52,53]. Depletion of glucose reduced the oxygen consumption rate of cancer cells, increased mitochondrial ROS generation, and caused apoptotic cancer cell death [48,50]. Low glucose levels triggered by ALESIA (Anticancer Ligand Enhancing Starvation-induced

Apoptosis) produced NADPH deficiency, which impairs the ability to defend against oxidative stress, ultimately resulting in apoptosis [42]. Upon glucose deprivation, activation of membrane-spanning 4-domains subfamily A (MS4A15)-associated Ca^{2+}-mediated cellular processes increased mitochondrial oxidative phosphorylation (OXPHOS) to rescue ovarian cancer cells from glucose-induced cell death. Consequently, increased ROS generation and low ATP production contribute to apoptotic cell death [30,54]. As a result, glucose restriction may be a promising anticancer treatment, with the production of ROS serving as a crucial mechanism of action.

In addition to ROS, apoptosis of human malignant mesothelioma cells cultured under glucose-depleted conditions was associated with a decrease in ATP levels [31,51]. When colon cancer cells were treated with 1% serum and low glucose, the expression of glucose transporters, GLUT1 and GLUT2, and glycolytic enzymes was suppressed, while the O_2 consumption rate of oxidative metabolism was increased, which finally resulted in a decrease in ATP synthesis [30]. The impairment of glucose transport was found to decrease mitochondrial respiration, oxidative phosphorylation, and glycolysis, resulting in a decrease in basal respiration and ATP generation [46]. Activation of phosphofructokinase-1-activated AMP-activated protein kinase (AMPK) is responsible for the decrease in ATP levels in A549 cancer cells after glucose deprivation [55]. Inhibition of glucose absorption by sodium glucose cotransporter-2 (SGLT-2) increases AMP/ATP ratios and inhibits ATP generation and oxidative phosphorylation, resulting in the activation of AMPK, which suppresses protein synthesis and cell proliferation [12].

During glucose deprivation, a compensatory response has been identified through increased p53-dependent fatty acid oxidation, hence providing substrate for ATP production through oxidative phosphorylation [56]. Oxidative stress in glucose starvation was ameliorated by the reduction of long-chain fatty acid synthesis from phosphorylation of acetyl-CoA carboxylase 1 (ACC1), while stimulating phosphorylated ACC2 to promote fatty acid oxidation, activating the long-chain fatty acid transporter carnitine palmitoyltransferase 1 (CPT1), and ultimately generating ATP and NADPH in non-small cell lung cancer cells. AMPK plays an important role in alleviating glucose starvation [57]. According to our findings, glucose deprivation was unable to cause the total death of all cancer cells, which may be a result of compensation responses to cellular oxidative stress.

Several studies have also demonstrated the metabolic compensation responses of cancer cells under glucose starvation, allowing the cell to survive in this harsh environment and preventing cell death. Glucose restriction activates the expression of nonessential amino acid transporters, providing an alternative energy source for cancer cells [58,59]. Glucose deprivation increases malic enzyme to provide NADPH for glutathione regeneration, resulting in ROS removal and a decrease in cancer cell death [52]. Reduced glucose availability increases the expression of HIF−1 and GLUT1 in lung cancer cells, triggering ROS production and eventually activating TGF−β, which promotes tumor development [60]. In addition, the absence of glucose-activated cell death was found to be attenuated by glutamine availability, which generated Krebs cycle intermediates that resulted in catalyzing redox reactions and strengthening the antioxidant system of cells [61,62]. Apoptosis induction by ginsenoside treatment in breast cancer cells demonstrated an increase in cell proliferation due to the activity of glutamine and its metabolites, glutamate, alanine, aspartate, and proline [63]. Thus, under glucose restriction, glutamine is considered to alleviate cell death, compensating for cell proliferation, migration, and invasion [63].

Under glucose restriction, cancer cells become more sensitive to anticancer therapies, enhancing treatment efficacy [64–66]. The apoptotic activity of metformin was augmented by the formation of ROS, which causes the loss of mitochondrial integrity under glucose starvation [67,68]. In addition, the apoptotic activity of oligomycin was dramatically enhanced in glucose-starved conditions via an excessive increase in mitochondrial ROS production upon inhibition of ATP synthase [60]. The synergistic effect of an erythrocyte membrane-biomimetic gas nanofactory and carbon monoxide therapy on the induction of the apoptosis process in tumors was observed under glucose starvation [69].

Fetal bovine serum has been determined to correlate with an apoptotic effect in cancer cells. According to our results, serum deprivation also caused apoptosis in HCT116 cells, which is consistent with previous research suggesting that serum deprivation has anticancer effects on a variety of cancer cells. Removing serum from culture media contributes to the depletion of fatty acids and growth factors [70]. Serum deprivation reduced cellular proliferation and increased apoptosis in cancer cells compared to those cultured on 10% FBS media and normal human cells [71–73]. ROS generation during serum deprivation has been identified as a mediator that triggers cancer cell apoptosis [74,75]. ROS formation in fasted serum was reported to result from a reduction in p67 subunits of NADPH oxidase for free radical antioxidant formation [76]. The mechanisms by which serum deprivation triggers apoptosis in cancer cells were discovered to involve a decrease in ATP synthesis leading to an inability to exchange ADP and ATP between mitochondria and cytosol and, eventually, hyperpolarization of the mitochondrial inner membrane [76]. The activation of apoptosis by the activation of fatty acid oxidation pathways in cancer cells was triggered by starvation-induced decreases in glucose absorption and ATP formation [77]. In addition, HepG2 cells deprived of serum synthesized more ketone bodies, resulting in a decrease in ATP levels [78].

Decreasing free fatty acid (FFA) levels following serum starvation treatment in acute myeloid leukemia cells demonstrated induction of apoptosis [79]. Endogenous fatty acid synthesis is required for tumor cell proliferation in human promyelocytic leukemia HL60 cells treated with serum- or fatty acid-free conditions [80]. After serum deprivation, accelerated fatty acid oxidation resulting from low fatty acid levels was found to trigger breast cancer cell death [72]. Consistent with glucose deprivation, however, it has been shown that cancer can adapt to cell stress under serum depletion by increasing ketone body catabolism to produce acetyl-CoA to enter the TCA cycle for ATP synthesis [78]. Several reports have demonstrated that the anticancer effect of cancer therapies is enhanced under serum deprivation treatment. By activating the ATM/Chk2/p53 signaling pathway, serum deprivation induced cancer cells to respond more to the drug cisplatin [81]. Similarly, serum fasting improved the anticancer activity of *Anemarrhena asphodeloides* extract against colon cancer cells [82].

C. gigantea extracts have been identified as an alternative for the effective treatment of a wide range of cancers [35,36,83–87]. Apoptotic induction by treatment with extracts from *C. gigantea* stem bark has been demonstrated to be mediated by activating ROS and fatty acids while inhibiting ATP production in colon cancer HCT116 cells [37]. The present study showed that in nutrient-depleted

media (both glucose and serum depletion), treatment of HCT116 cells with the CGDCM extract fraction from *C. gigantea* stem bark at concentrations lower than the IC50 showed a stronger anticancer effect than in complete medium. It was clearly demonstrated that, in conjunction with nutrient deprivation, treatment of HCT116 cells with the extract enhanced apoptosis, in correlation with increased ROS generation, and inhibited fatty acid and ATP supply. Our results suggest that the extract and nutrient deprivation-induced anti-proliferative and apoptotic responses target the same common mechanisms underlying their anticancer effectiveness.

For the future application of *C. gigantea* extracts as a potentially effective alternative anticancer agent, it may be necessary to investigate the effects of *C. gigantea* extracts and nutrient deprivation on an additional type of cancer cell. In addition to ROS, ATP, and fatty acid levels, it is necessary to identify the mechanisms that correspond to cancer apoptosis via metabolic pathways. Additionally, it may be beneficial to investigate the combined effects of CGDCM and food deprivation on animal models as part of ongoing research. Comparing the anticancer effects of dietary restriction in animals to those of serum deprivation in cell models will establish a unique mechanism of action. In addition, an in vivo model is necessary to investigate the deleterious effects of nutrient deprivation that enhance the anticancer effect of CGDCM.

We conclude that the CGDCM extract fraction of *C. gigantea* stem bark is proposed for effective anticancer treatment, and its improved effectiveness during food deprivation may provide a basis for the development of promising anticancer regimens in the future.

Author contribution statement

O.S.: Formal analysis, Investigation, Methodology, Software, Validation, Visualization, Writing - original draft, and Writing - review & editing.

D.P.: Data curation, Formal analysis, Investigation, Methodology, Software, Validation, Visualization, Writing - original draft, and Writing - review & editing.

J.S.: Writing - review & editing.

A.W.: Writing - review & editing.

M.S.: Writing - review & editing.

N.K.: Formal analysis, Methodology, Software, Validation, Visualization.

S.P.: Conceptualization, Data curation, Formal analysis, Funding acquisition, Investigation, Methodology, Software, Validation, Visualization, Writing - original draft, and Writing - review & editing.

P.S.: Conceptualization, Data curation, Formal analysis, Funding acquisition, Investigation, Methodology, Software, Validation, Visualization, Writing - original draft, and Writing - review & editing.

Funding sources

This work was supported by National Science Research and Innovation Fund (NSRF) of Thailand [Grant NO. R2564B007 to S.P. and P.S. and R2564B033 to A.W.], the Agricultural Research Development Agency (Public Organization), Thailand [Grant NO. CRP6505030030 to S.P.], and the graduate thesis funding from the Department of Physiology, Faculty of Medical Science, Naresuan University, Phitsanulok, Thailand [Grant NO.62063645 to O.S.]. The funders had no role in study design, data collection and analysis, decision to publish, or preparation of the manuscript.

Data availability statement

No data was used for the research described in the article.

Declaration of competing interest

The authors declare that they have no known competing financial interests or personal relationships that could have appeared to influence the work reported in this paper.

References

[1] H. Sung, J. Ferlay, R.L. Siegel, M. Laversanne, I. Soerjomataram, A. Jemal, F. Bray, Global cancer statistics 2020: GLOBOCAN estimates of incidence and mortality worldwide for 36 cancers in 185 countries, CA A Cancer J. Clin. 71 (2021) 209–249, https://doi.org/10.3322/caac.21660.

[2] M. Riihimäki, A. Hemminki, J. Sundquist, K. Hemminki, Patterns of metastasis in colon and rectal cancer, Sci. Rep. 6 (2016), 29765, https://doi.org/10.1038/srep29765.

[3] P. Rawla, T. Sunkara, A. Barsouk, Epidemiology of colorectal cancer: incidence, mortality, survival, and risk factors, Gastroenterol. Rev. 14 (2019) 89–103, https://doi.org/10.5114/pg.2018.81072.

[4] S. Senapati, A.K. Mahanta, S. Kumar, P. Maiti, Controlled drug delivery vehicles for cancer treatment and their performance, Signal Transduct. Targeted Ther. 3 (2018) 7, https://doi.org/10.1038/s41392-017-0004-3.

[5] Y. Wang, Y. Xia, Z. Lu, Metabolic features of cancer cells, Cancer Commun. 38 (2018) 65, https://doi.org/10.1186/s40880-018-0335-7.

[6] M. Coelho, T. Oliveira, R. Fernandes, State of the art paper Biochemistry of adipose tissue: an endocrine organ, Arch. Med. Sci. 2 (2013) 191–200, https://doi.org/10.5114/aoms.2013.33181.

[7] H. Schulz, Fatty acid oxidation, in: Encyclopedia of Biological Chemistry, Elsevier, 2013, pp. 281–284, https://doi.org/10.1016/B978-0-12-378630-2.00071-2.

[8] C. de Carvalho, M. Caramujo, The various roles of fatty acids, Molecules 23 (2018) 2583, https://doi.org/10.3390/molecules23102583.

[9] M. Chen, J. Huang, The expanded role of fatty acid metabolism in cancer: new aspects and targets, Precis. Clin. Med. 2 (2019) 183–191, https://doi.org/10.1093/pcmedi/pbz017.

[10] Y. Cui, J. Peng, M. Zheng, H. Ge, X. Wu, Y. Xia, Y. Huang, S. Wang, Y. Yin, Z. Fu, H. Xie, TRPC5OS induces tumorigenesis by increasing ENO1-mediated glucose uptake in breast cancer, Transl. Oncol. 22 (2022), 101447, https://doi.org/10.1016/j.tranon.2022.101447.

[11] H. Li, L. Fu, B. Liu, X. Lin, Q. Dong, E. Wang, Ajuba overexpression regulates mitochondrial potential and glucose uptake through YAP/Bcl-xL/GLUT1 in human gastric cancer, Gene 693 (2019) 16–24, https://doi.org/10.1016/j.gene.2019.01.018.

[12] J. Zhou, J. Zhu, S.-J. Yu, H.-L. Ma, J. Chen, X.-F. Ding, G. Chen, Y. Liang, Q. Zhang, Sodium-glucose co-transporter-2 (SGLT-2) inhibition reduces glucose uptake to induce breast cancer cell growth arrest through AMPK/mTOR pathway, Biomed. Pharmacother. 132 (2020), 110821, https://doi.org/10.1016/j.biopha.2020.110821.

[13] K. Kaji, N. Nishimura, K. Seki, S. Sato, S. Saikawa, K. Nakanishi, M. Furukawa, H. Kawaratani, M. Kitade, K. Moriya, T. Namisaki, H. Yoshiji, Sodium glucose cotransporter 2 inhibitor canagliflozin attenuates liver cancer cell growth and angiogenic activity by inhibiting glucose uptake, Int. J. Cancer 142 (2018) 1712–1722, https://doi.org/10.1002/ijc.31193.

[14] J. Krstic, I. Reinisch, K. Schindlmaier, M. Galhuber, Z. Riahi, N. Berger, N. Kupper, E. Moyschewitz, M. Auer, H. Michenthaler, C. Nössing, M.R. Depaoli, J. Ramadani-Muja, S. Usluer, S. Stryeck, M. Pichler, B. Rinner, A.J.A. Deutsch, A. Reinisch, T. Madl, R.Z. Chiozzi, A.J.R. Heck, M. Huch, R. Malli, A. Prokesch, Fasting improves therapeutic response in hepatocellular carcinoma through p53-dependent metabolic synergism, Sci. Adv. 8 (2022), https://doi.org/10.1126/sciadv.abh2635.

[15] J. Yu, Z. Wei, Q. Li, F. Wan, Z. Chao, X. Zhang, L. Lin, H. Meng, L. Tian, Advanced cancer starvation therapy by simultaneous deprivation of lactate and glucose using a MOF nanoplatform, Adv. Sci. 8 (2021), 2101467, https://doi.org/10.1002/advs.202101467.

[16] W. Zhang, K. Liu, Y. Pei, J. Ma, J. Tan, J. Zhao, Mst1 regulates non-small cell lung cancer A549 cell apoptosis by inducing mitochondrial damage via ROCK1/F−actin pathways, Int. J. Oncol. (2018), https://doi.org/10.3892/ijo.2018.4586.

[17] G. di Conza, S. Trusso Cafarello, X. Zheng, Q. Zhang, M. Mazzone, PHD2 targeting overcomes breast cancer cell death upon glucose starvation in a PP2A/B55α-mediated manner, Cell Rep. 18 (2017) 2836–2844, https://doi.org/10.1016/j.celrep.2017.02.081.

[18] J. Zhao, Y. Chen, F. Liu, M. Yin, Overexpression of miRNA-143 inhibits colon cancer cell proliferation by inhibiting glucose uptake, Arch. Med. Res. 49 (2018) 497–503, https://doi.org/10.1016/j.arcmed.2018.12.009.

[19] R. Tang, A. Kimishima, A. Setiawan, M. Arai, Secalonic acid D as a selective cytotoxic substance on the cancer cells adapted to nutrient starvation, J. Nat. Med. 74 (2020) 495–500, https://doi.org/10.1007/s11418-020-01390-0.

[20] L. Raffaghello, C. Lee, F.M. Safdie, M. Wei, F. Madia, G. Bianchi, V.D. Longo, Starvation-dependent differential stress resistance protects normal but not cancer cells against high-dose chemotherapy, Proc. Natl. Acad. Sci. USA 105 (2008) 8215–8220, https://doi.org/10.1073/pnas.0708100105.

[21] A.C. Ferretti, F. Hidalgo, F.M. Tonucci, E. Almada, A. Pariani, M.C. Larocca, C. Favre, Metformin and glucose starvation decrease the migratory ability of hepatocellular carcinoma cells: targeting AMPK activation to control migration, Sci. Rep. 9 (2019) 2815, https://doi.org/10.1038/s41598-019-39556-w.

[22] S. Aminzadeh-Gohari, R.G. Feichtinger, B. Kofler, Energy metabolism and metabolic targeting of neuroblastoma, in: Neuroblastoma, Elsevier, 2019, pp. 113–132, https://doi.org/10.1016/B978-0-12-812005-7.00007-2.

[23] L.S. Pike, A.L. Smift, N.J. Croteau, D.A. Ferrick, M. Wu, Inhibition of fatty acid oxidation by etomoxir impairs NADPH production and increases reactive oxygen species resulting in ATP depletion and cell death in human glioblastoma cells, Biochim. Biophys. Acta Bioenerg. 1807 (2011) 726–734, https://doi.org/10.1016/j.bbabio.2010.10.022.

[24] I. Samudio, R. Harmancey, M. Fiegl, H. Kantarjian, M. Konopleva, B. Korchin, K. Kaluarachchi, W. Bornmann, S. Duvvuri, H. Taegtmeyer, M. Andreeff, Pharmacologic inhibition of fatty acid oxidation sensitizes human leukemia cells to apoptosis induction, J. Clin. Invest. 120 (2010) 142–156, https://doi.org/10.1172/JCI38942.

[25] B. Schroeder, T. vander Steen, I. Espinoza, C.M.K. Venkatapoorna, Z. Hu, F.M. Silva, K. Regan, E. Cuyàs, X.W. Meng, S. Verdura, A. Arbusà, P.A. Schneider, K. S. Flatten, G. Kemble, J. Montero, S.H. Kaufmann, J.A. Menendez, R. Lupu, Fatty acid synthase (FASN) regulates the mitochondrial priming of cancer cells, Cell Death Dis. 12 (2021) 977, https://doi.org/10.1038/s41419-021-04262-x.

[26] S. Al-Bahlani, H. Al-Lawati, M. Al-Adawi, N. Al-Abri, B. Al-Dhahli, K. Al-Adawi, Fatty acid synthase regulates the chemosensitivity of breast cancer cells to cisplatin-induced apoptosis, Apoptosis 22 (2017) 865–876, https://doi.org/10.1007/s10495-017-1366-2.

[27] Y. Yan, Y. Zhou, J. Li, Z. Zheng, Y. Hu, L. Li, W. Wu, Sulforaphane downregulated fatty acid synthase and inhibited microtubule-mediated mitophagy leading to apoptosis, Cell Death Dis. 12 (2021) 917, https://doi.org/10.1038/s41419-021-04198-2.

[28] G. Gstraunthaler, Alternatives to the use of fetal bovine serum: serum-free cell culture, ALTEX (2003) 257–281, https://doi.org/10.14573/altex.2003.4.257.

[29] M. Hamada, H. Inaba, K. Nishiyama, S. Yoshida, Y. Yura, M. Matsumoto-Nakano, N. Uzawa, Prognostic association of starvation-induced gene expression in head and neck cancer, Sci. Rep. 11 (2021), 19130, https://doi.org/10.1038/s41598-021-98544-1.

[30] G. Bianchi, R. Martella, S. Ravera, C. Marini, S. Capitanio, A. Orengo, L. Emionite, C. Lavarello, A. Amaro, A. Petretto, U. Pfeffer, G. Sambuceti, V. Pistoia, L. Raffaghello, V.D. Longo, Fasting induces anti-Warburg effect that increases respiration but reduces ATP-synthesis to promote apoptosis in colon cancer models, Oncotarget 6 (2015) 11806–11819, https://doi.org/10.18632/oncotarget.3688.

[31] F. Ciampi, L.M. Sordillo, J.C. Gandy, M. Caroprese, A. Sevi, M. Albenzio, A. Santillo, Evaluation of natural plant extracts as antioxidants in a bovine in vitro model of oxidative stress, J. Dairy Sci. 103 (2020) 8938–8947, https://doi.org/10.3168/jds.2020-18182.

[32] M. Kadiyala, S. Ponnusankar, K. Elango, Calotropis gigantiea (L.) R. Br (Apocynaceae): a phytochemical and pharmacological review, J. Ethnopharmacol. 150 (2013) 32–50, https://doi.org/10.1016/j.jep.2013.08.045.

[33] I.N. Khan, MdM.I. Sarker, M. Ajrin, Sedative and anxiolytic effects of ethanolic extract of *Calotropis gigantea* (Asclepiadaceae) leaves, Asian Pac. J. Trop. Biomed. 4 (2014), https://doi.org/10.12980/APJTB.4.2014C1147. S400–S404.

[34] M.R. Habib, M.R. karim, Evaluation of antitumour activity of *Calotropis gigantea* L. root bark against Ehrlich ascites carcinoma in Swiss albino mice, Asian Pac. J. Tropical Med. 4 (2011) 786–790, https://doi.org/10.1016/S1995-7645(11)60194-6.

[35] C. Seeka, S. Sutthivaiyakit, Cytotoxic cardenolides from the leaves of *Calotropis gigantea*, Chem. Pharm. Bull. 58 (2010) 725–728, https://doi.org/10.1248/cpb.58.725.

[36] J. Lee, H.-J. Jang, H. Chun, T.-H. Pham, Y. Bak, J.-W. Shin, H. Jin, Y.-I. Kim, H.W. Ryu, S.R. Oh, D.-Y. Yoon, *Calotropis gigantea* extract induces apoptosis through extrinsic/intrinsic pathways and reactive oxygen species generation in A549 and NCI-H1299 non-small cell lung cancer cells, BMC Compl. Alternative Med. 19 (2019) 134, https://doi.org/10.1186/s12906-019-2561-1.

[37] T. Winitchaikul, S. Sawong, D. Surangkul, M. Srikummool, J. Somran, D. Pekthong, K. Kamonlakorn, P. Nangngam, S. Parhira, P. Srisawang, *Calotropis gigantea* stem bark extract induced apoptosis related to ROS and ATP production in colon cancer cells, PLoS One 16 (2021), e0254392, https://doi.org/10.1371/journal.pone.0254392.

[38] E. Gottlieb, S.M. Armour, M.H. Harris, C.B. Thompson, Mitochondrial membrane potential regulates matrix configuration and cytochrome c release during apoptosis, Cell Death Differ. 10 (2003) 709–717, https://doi.org/10.1038/sj.cdd.4401231.

[39] F.J. Bock, S.W.G. Tait, Mitochondria as multifaceted regulators of cell death, Nat. Rev. Mol. Cell Biol. 21 (2020) 85–100, https://doi.org/10.1038/s41580-019-0173-8.

[40] S. Sawong, D. Pekthong, P. Suknoppakit, T. Winitchaikul, W. Kaewkong, J. Somran, C. Intapa, S. Parhira, P. Srisawang, *Calotropis gigantea* stem bark extracts inhibit liver cancer induced by diethylnitrosamine, Sci. Rep. 12 (2022), 12151, https://doi.org/10.1038/s41598-022-16321-0.

[41] J. Fan, D. Ren, J. Wang, X. Liu, H. Zhang, M. Wu, G. Yang, Bruceine D induces lung cancer cell apoptosis and autophagy via the ROS/MAPK signaling pathway in vitro and in vivo, Cell Death Dis. 11 (2020) 126, https://doi.org/10.1038/s41419-020-2317-3.

[42] M. Toyomoto, A. Inoue, K. Iida, M. Denawa, I. Kii, F.M. Ngako Kadji, T. Kishi, D. Im, T. Shimamura, H. Onogi, S. Yoshida, S. Iwata, J. Aoki, T. Hosoya, M. Hagiwara, S1PR3–G12-biased agonist ALESIA targets cancer metabolism and promotes glucose starvation, Cell Chem. Biol. 28 (2021) 1132–1144.e9, https://doi.org/10.1016/j.chembiol.2021.01.004.

[43] A. Hirayama, K. Kami, M. Sugimoto, M. Sugawara, N. Toki, H. Onozuka, T. Kinoshita, N. Saito, A. Ochiai, M. Tomita, H. Esumi, T. Soga, Quantitative metabolome profiling of colon and stomach cancer microenvironment by capillary electrophoresis time-oF−flight mass spectrometry, Cancer Res. 69 (2009) 4918–4925, https://doi.org/10.1158/0008-5472.CAN-08-4806.

[44] C. Huang, S. Sheng, R. Li, X. Sun, J. Liu, G. Huang, Lactate promotes resistance to glucose starvation via upregulation of Bcl-2 mediated by mTOR activation, Oncol. Rep. 33 (2015) 875–884, https://doi.org/10.3892/or.2014.3655.

[45] C. Zhou, W. Qian, J. Li, J. Ma, X. Chen, Z. Jiang, L. Cheng, W. Duan, Z. Wang, Z. Wu, Q. Ma, X. Li, High glucose microenvironment accelerates tumor growth via SREBP1-autophagy axis in pancreatic cancer, J. Exp. Clin. Cancer Res. 38 (2019) 302, https://doi.org/10.1186/s13046-019-1288-7.

[46] C. Garlapati, S. Joshi, R.C. Turaga, M. Mishra, M.D. Reid, S. Kapoor, L. Artinian, V. Rehder, R. Aneja, Monoethanolamine-induced glucose deprivation promotes apoptosis through metabolic rewiring in prostate cancer, Theranostics 11 (2021) 9089–9106, https://doi.org/10.7150/thno.62724.

[47] A. Nasir Kansestani, K. Mansouri, S. Hemmati, M. Erfan Zare, A. Mostafaie, High glucose-reduced apoptosis in human breast cancer cells is mediated by activation of NF−κB, Iran. J. Allergy, Asthma Immunol. (2019), https://doi.org/10.18502/ijaai.v18i2.918.

[48] W. Sa-nongdej, S. Chongthammakun, C. Songthaveesin, Nutrient starvation induces apoptosis and autophagy in C6 glioma stem-like cells, Heliyon 7 (2021), e06352, https://doi.org/10.1016/j.heliyon.2021.e06352.

[49] L. Ma, J. Wei, J. Wan, W. Wang, L. Wang, Y. Yuan, Z. Yang, X. Liu, L. Ming, Low glucose and metformin-induced apoptosis of human ovarian cancer cells is connected to ASK1 via mitochondrial and endoplasmic reticulum stress-associated pathways, J. Exp. Clin. Cancer Res. 38 (2019) 77, https://doi.org/10.1186/s13046-019-1090-6.

[50] G.K. Raut, M. Chakrabarti, D. Pamarthy, M.P. Bhadra, Glucose starvation-induced oxidative stress causes mitochondrial dysfunction and apoptosis via Prohibitin 1 upregulation in human breast cancer cells, Free Radic. Biol. Med. 145 (2019) 428–441, https://doi.org/10.1016/j.freeradbiomed.2019.09.020.

[51] S. Hwang, M. Kim, S. Ji, Y. Yang, Y. Jeong, Y. Kim, Glucose starvation induces resistance to metformin through the elevation of mitochondrial multidrug resistance protein 1, Cancer Sci. 110 (2019) 1256–1267, https://doi.org/10.1111/cas.13952.

[52] Y.-X. Lu, H.-Q. Ju, Z.-X. Liu, D.-L. Chen, Y. Wang, Q. Zhao, Q.-N. Wu, Z. Zeng, H.-B. Qiu, P.-S. Hu, Z.-Q. Wang, D.-S. Zhang, F. Wang, R.-H. Xu, ME1 regulates NADPH homeostasis to promote gastric cancer growth and metastasis, Cancer Res. 78 (2018) 1972–1985, https://doi.org/10.1158/0008-5472.CAN-17-3155.

[53] A.C. Ferretti, F.M. Tonucci, F. Hidalgo, E. Almada, M.C. Larocca, C. Favre, AMPK and PKA interaction in the regulation of survival of liver cancer cells subjected to glucose starvation, Oncotarget 7 (2016) 17815–17828, https://doi.org/10.18632/oncotarget.7404.

[54] Y. Fang, H. Yu, H. Zhou, MS4A15 acts as an oncogene in ovarian cancer through reprogramming energy metabolism, Biochem. Biophys. Res. Commun. 598 (2022) 47–54, https://doi.org/10.1016/j.bbrc.2022.01.128.

[55] P.-P. Liu, J. Liao, Z.-J. Tang, W.-J. Wu, J. Yang, Z.-L. Zeng, Y. Hu, P. Wang, H.-Q. Ju, R.-H. Xu, P. Huang, Metabolic regulation of cancer cell side population by glucose through activation of the Akt pathway, Cell Death Differ. 21 (2014) 124–135, https://doi.org/10.1038/cdd.2013.131.

[56] D. Jiang, E.L. LaGory, D. Kenzelmann Brož, K.T. Bieging, C.A. Brady, N. Link, J.M. Abrams, A.J. Giaccia, L.D. Attardi, Analysis of p53 transactivation domain mutants reveals Acad11 as a metabolic target important for p53 pro-survival function, Cell Rep. 10 (2015) 1096–1109, https://doi.org/10.1016/j.celrep.2015.01.043.

[57] J. Chen, L. Zou, G. Lu, O. Grinchuk, L. Fang, D.S.T. Ong, R. Taneja, C.-N. Ong, H.-M. Shen, PFKP alleviates glucose starvation-induced metabolic stress in lung cancer cells via AMPK-ACC2 dependent fatty acid oxidation, Cell Discovery 8 (2022) 52, https://doi.org/10.1038/s41421-022-00406-1.

[58] G. Wang, L. Dai, L. Luo, W. Xu, C. Zhang, Y. Zhu, Z. Chen, W. Hu, X. Xu, W. Pan, Non-essential amino acids attenuate apoptosis of gastric cancer cells induced by glucose starvation, Oncol. Rep. 32 (2014) 332–340, https://doi.org/10.3892/or.2014.3205.

[59] J. Tan, H.-L. Wang, J. Yang, Q.-Q. Liu, C.-M. Li, Y.-Q. Wang, L.-N. Fu, Q.-Y. Gao, Y.-X. Chen, J.-Y. Fang, JMJD2B-induced amino acid alterations enhance the survival of colorectal cancer cells under glucose-deprivation via autophagy, Theranostics 10 (2020) 5763–5777, https://doi.org/10.7150/thno.38087.

[60] S.-H. Hwang, Y. Yang, J.-H. Jung, Y. Kim, Heterogeneous response of cancer-associated fibroblasts to the glucose deprivation through mitochondrial calcium uniporter, Exp. Cell Res. 406 (2021), 112778, https://doi.org/10.1016/j.yexcr.2021.112778.

[61] I. Chiodi, G. Picco, C. Martino, C. Mondello, Cellular response to glutamine and/or glucose deprivation in in vitro transformed human fibroblasts, Oncol. Rep. (2019), https://doi.org/10.3892/or.2019.7125.

[62] M. Yuneva, N. Zamboni, P. Oefner, R. Sachidanandam, Y. Lazebnik, Deficiency in glutamine but not glucose induces MYC-dependent apoptosis in human cells, J. Cell Biol. 178 (2007) 93–105, https://doi.org/10.1083/jcb.200703099.

[63] B. Zhang, R. Fu, Z. Duan, S. Shen, C. Zhu, D. Fan, Ginsenoside CK induces apoptosis in triple-negative breast cancer cells by targeting glutamine metabolism, Biochem. Pharmacol. 202 (2022), 115101, https://doi.org/10.1016/j.bcp.2022.115101.

[64] H. Wen, Y. Fei, R. Cai, X. Yao, Y. Li, X. Wang, C. Xue, Y. Hu, M. Li, Z. Luo, Tumor-activatable biomineralized nanotherapeutics for integrative glucose starvation and sensitized metformin therapy, Biomaterials 278 (2021), 121165, https://doi.org/10.1016/j.biomaterials.2021.121165.

[65] X. Meng, Z. Lu, Q. Lv, Y. Jiang, L. Zhang, Z. Wang, Tumor metabolism destruction via metformin-based glycolysis inhibition and glucose oxidase-mediated glucose deprivation for enhanced cancer therapy, Acta Biomater. 145 (2022) 222–234, https://doi.org/10.1016/j.actbio.2022.04.022.

[66] X. Li, C. Jiang, Q. Wang, S. Yang, Y. Cao, J. Hao, D. Niu, Y. Chen, B. Han, X. Jia, P. Zhang, Y. Li, A "valve-closing" starvation strategy for amplification of tumor-specific chemotherapy, Adv. Sci. 9 (2022), 2104671, https://doi.org/10.1002/advs.202104671.

[67] S. Scotland, E. Saland, N. Skuli, F. de Toni, H. Boutzen, E. Micklow, I. Sénégas, R. Peyraud, L. Peyriga, F. Théodoro, E. Dumon, Y. Martineau, G. Danet-Desnoyers, F. Bono, C. Rocher, T. Levade, S. Manenti, C. Junot, J.-C. Portais, N. Alet, C. Récher, M.A. Selak, M. Carroll, J.-E. Sarry, Mitochondrial energetic and AKT status mediate metabolic effects and apoptosis of metformin in human leukemic cells, Leukemia 27 (2013) 2129–2138, https://doi.org/10.1038/leu.2013.107.

[68] R. Aoun, C. el Hadi, R. Tahtouh, R. el Habre, G. Hilal, Microarray analysis of breast cancer gene expression profiling in response to 2-deoxyglucose, metformin, and glucose starvation, Cancer Cell Int. 22 (2022) 123, https://doi.org/10.1186/s12935-022-02542-w.

[69] Y. Wang, Z. Liu, H. Wang, Z. Meng, Y. Wang, W. Miao, X. Li, H. Ren, Starvation-amplified CO generation for enhanced cancer therapy via an erythrocyte membrane-biomimetic gas nanofactory, Acta Biomater. 92 (2019) 241–253, https://doi.org/10.1016/j.actbio.2019.05.009.

[70] C.J. Schamberger, C. Gerner, C. Cerni, bFGF rescues 423-cells from serum starvation-induced apoptosis downstream of activated caspase-3, FEBS Lett. 573 (2004) 19–25, https://doi.org/10.1016/j.febslet.2004.07.053.

[71] Y. Huang, Z. Fu, W. Dong, Z. Zhang, J. Mu, J. Zhang, Serum starvation-induces down-regulation of Bcl-2/Bax confers apoptosis in tongue coating-related cells in vitro, Mol. Med. Rep. (2018), https://doi.org/10.3892/mmr.2018.8512.

[72] S.C. Kwong, A.H.A. Jamil, A. Rhodes, N.A. Taib, I. Chung, Metabolic role of fatty acid binding protein 7 in mediating triple-negative breast cancer cell death via PPAR-α signaling, J. Lipid Res. 60 (2019) 1807–1817, https://doi.org/10.1194/jlr.M092379.

[73] F. Papa, S. Scacco, R. Vergari, M. de Benedittis, M. Petruzzi, L.L. Muzio, R. Serpico, Expression and subcellular distribution of Bcl-2 and BAX proteins in serum-starved human keratinocytes and mouth carcinoma epidermoid cultures, Life Sci. 73 (2003) 2865–2872, https://doi.org/10.1016/S0024-3205(03)00706-9.

[74] S.B. Lee, J.J. Kim, T.W. Kim, B.S. Kim, M.-S. Lee, Y. do Yoo, Serum deprivation-induced reactive oxygen species production is mediated by Romo1, Apoptosis 15 (2010) 204–218, https://doi.org/10.1007/s10495-009-0411-1.

[75] N. Zheng, K. Wang, J. He, Y. Qiu, G. Xie, M. Su, W. Jia, H. Li, Effects of ADMA on gene expression and metabolism in serum-starved LoVo cells, Sci. Rep. 6 (2016), 25892, https://doi.org/10.1038/srep25892.

[76] C. Yang, S.-H. Jo, B. Csernus, E. Hyjek, Y. Liu, A. Chadburn, Y.L. Wang, Activation of peroxisome proliferator-activated receptor γ contributes to the survival of T lymphoma cells by affecting cellular metabolism, Am. J. Pathol. 170 (2007) 722–732, https://doi.org/10.2353/ajpath.2007.060651.

[77] K. Liu, F. Li, Q. Sun, N. Lin, H. Han, K. You, F. Tian, Z. Mao, T. Li, T. Tong, M. Geng, Y. Zhao, W. Gu, W. Zhao, p53 β-hydroxybutyrylation attenuates p53 activity, Cell Death Dis. 10 (2019) 243, https://doi.org/10.1038/s41419-019-1463-y.

[78] D. Huang, T. Li, L. Wang, L. Zhang, R. Yan, K. Li, S. Xing, G. Wu, L. Hu, W. Jia, S.-C. Lin, C. v Dang, L. Song, P. Gao, H. Zhang, Hepatocellular carcinoma redirects to ketolysis for progression under nutrition deprivation stress, Cell Res. 26 (2016) 1112–1130, https://doi.org/10.1038/cr.2016.109.

[79] Y. Tabe, S. Yamamoto, K. Saitoh, K. Sekihara, N. Monma, K. Ikeo, K. Mogushi, M. Shikami, V. Ruvolo, J. Ishizawa, N. Hail, S. Kazuno, M. Igarashi, H. Matsushita, Y. Yamanaka, H. Arai, I. Nagaoka, T. Miida, Y. Hayashizaki, M. Konopleva, M. Andreeff, Bone marrow adipocytes facilitate fatty acid oxidation activating AMPK

and a transcriptional network supporting survival of acute monocytic leukemia cells, Cancer Res. 77 (2017) 1453–1464, https://doi.org/10.1158/0008-5472.CAN-16-1645.

[80] E.S. Pizer, F.D. Wood, G.R. Pasternack, F.P. Kuhajda, Fatty acid synthase (FAS): a target for cytotoxic antimetabolites in HL60 promyelocytic leukemia cells, Cancer Res. 56 (1996) 745–751.

[81] Y. Shi, E. Felley-Bosco, T.M. Marti, K. Orlowski, M. Pruschy, R.A. Stahel, Starvation-induced activation of ATM/Chk2/p53 signaling sensitizes cancer cells to cisplatin, BMC Cancer 12 (2012) 571, https://doi.org/10.1186/1471-2407-12-571.

[82] K.-Y. Ji, K.M. Kim, Y.H. Kim, K.-S. Shim, J.Y. Lee, T. Kim, S. Chae, Serum starvation sensitizes anticancer effect of Anemarrhena asphodeloides via p38/JNK-induced cell cycle arrest and apoptosis in colorectal cancer cells, Am. J. Chin. Med. 49 (2021) 1001–1016, https://doi.org/10.1142/S0192415X21500488.

[83] M.R. Habib, M.R. Karim, Effect of anhydrosophoradiol-3-acetate of *Calotropis gigantea* (Linn.) flower as antitumoric agent against Ehrlich's ascites carcinoma in mice, Pharmacol. Rep. 65 (2013) 761–767, https://doi.org/10.1016/S1734-1140(13)71057-0.

[84] R. Mutiah, Sukardiman, A. Widyawaruyanti, Cytotoxic effect of crude extract and fraction from calotropis gigantea leaves on human colon cancer WIDR cell lines, Int. J. Pharm. Pharmaceut. Sci. 9 (2016) 83, https://doi.org/10.22159/ijpps.2017v9i1.9022.

[85] K.D.H. Nguyen, P.H. Dang, H.X. Nguyen, M.T.T. Nguyen, S. Awale, N.T. Nguyen, Phytochemical and cytotoxic studies on the leaves of *Calotropis gigantea*, Bioorg. Med. Chem. Lett 27 (2017) 2902–2906, https://doi.org/10.1016/j.bmcl.2017.04.087.

[86] K.R. Kharat, A.S. Kharat, The *calotropis gigantea* methanolic extract induces apoptosis in human breast carcinoma cells, Iran. J. Med. Sci. 44 (2019) 483–492, https://doi.org/10.30476/ijms.2019.44966.

[87] R. Mutiah, A. Widyawaruyanti, S. Sukardiman, Calotroposid A: a glycosides terpenoids from *Calotropis gigantea* induces apoptosis of colon cancer WiDr cells through cell cycle arrest G2/M and caspase 8 expression, Asian Pac. J. Cancer Prev. APJCP 19 (2018) 1457–1464, https://doi.org/10.22034/APJCP.2018.19.6.1457.